JPET Fast Forward. Published on July 21, 2009 as DOI: 10.1124/jpet.109.155705

JPET #155705

Abrogation of MAPK and Akt Signaling by Vandetanib (ZACTIMA™)[§] Synergistically Potentiates Histone Deacetylase Inhibitor-Induced Apoptosis in Human Glioma Cells

Esther P. Jane, Daniel R. Premkumar, Steven O. Addo-Yobo, and Ian F. Pollack

Department of Neurosurgery (E.P.J., D.R.P., I.F.P.), University of Pittsburgh School of Medicine (E.P.J., D.R.P., S.O.A., I.F.P.), University of Pittsburgh Cancer Institute Brain Tumor Center (I.F.P.), Pittsburgh, Pennsylvania.

JPET Fast Forward. Published on July 21, 2009 as DOI: 10.1124/jpet.109.155705
This article has not been copyedited and formatted. The final version may differ from this version.

Running title: Synergistic augmentation of vandetanib-induced cytotoxicity

Address correspondence to:
Ian F. Pollack, M.D., F.A.C.S., F.A.A.P.
Department of Neurosurgery,
Children's Hospital Drive,
45th Street and Penn Avenue,
Pittsburgh, PA 15201.
Telephone: 412-692-5881
Fax: 412-692-5921
E-mail: ian.pollack@chp.edu

Total number of text pages: 32

Number of tables: 1

Number of figures: 8

Number of references: 40

Number of words in Abstract: 216

Number of words in Introduction: 663

Number of words in Discussion: 792

ABBREVIATIONS: MAPK, mitogen-activated protein kinase; ERK, extracellular signal-regulated kinase; EGF, epidermal growth factor; EGFR, epidermal growth factor receptor; PDGF, platelet derived growth factor; PDGFR, platelet-derived growth factor receptor; VEGF, vascular endothelial growth factor; VEGFR, vascular endothelial growth factor receptor; DMSO, dimethyl sulfoxide; HDAC, histone deacetylase; HDACI, histone deacetylase inhibitor; MTS, 3-[4,5-dimethylthiazol- 2yl]-5-[3-carboxymethoxyphenyl]-2-[4-sulfophenyl]-2*H*, tetrazolium; FITC, fluorescein isothiocyanate; PBS, phosphate-buffered saline; PAGE, polyacrylamide gel electrophoresis; TBS, Tris-buffered saline; RTK, receptor tyrosine kinase; TKI, tyrosine kinase inhibitor; CDK, cyclin-dependent kinase; PI3K, phosphatidylinositol 3-kinase; E-64, *N*-(*trans*-epoxysuccinyl)-L-leucine 4-guanidinobutylamide; SAHA, suberoylanalide hydroxamic acid; TSA, trichostatin A.

ABSTRACT

Vandetanib is a multitargeted tyrosine kinase inhibitor. Our initial studies demonstrated that this agent blocks vascular endothelial growth factor receptor (VEGFR), epidermal growth factor receptor (EGFR), and platelet-derived growth factor receptor (PDGFR) phosphorylation and MAPK-mediated signaling in glioma cell lines in a dose-dependent manner. Despite these effects, we observed that vandetanib had little effect on apoptosis induction at clinically achievable concentrations. Because histone deacetylase inhibitors (HDACI) have been suggested to regulate signaling protein transcription and downstream interactions via modulation of protein chaperone function through Hsp90, we investigated whether combining vandetanib with an HDACI could synergistically potentiate signaling pathway inhibition and apoptosis induction in a panel of malignant human glioma cell lines. Proliferation assays, apoptosis induction studies, and Western immunoblot analysis were conducted in cells treated with vandetanib and HDACIs as single agents or in combination. Vandetanib and SAHA reduced proliferation in all cell lines when used as single agents, and the combination produced marked potentiation of growth inhibition as assessed by combinatorial methods. These effects were paralleled by potentiation of Akt signaling inhibition and apoptosis induction. Our results indicate that inhibition of histone deacetylation enhances the antiproliferative effect of vandetanib in malignant human glioma cell lines by enhancing inhibition of MAPK, Akt and other downstream effectors which may have application in combinatorial therapeutics for these tumors.

INTRODUCTION

Glioblastoma multiforme (GBM) is characterized by rapid disease progression despite aggressive surgical resection, irradiation, and administration of conventional chemotherapy. However, recent molecular studies have identified a variety of growth factor receptors instrumental in glioma tumorigenesis that may constitute novel therapeutic targets. Epidermal growth factor receptor (EGFR) amplification and constitutive activation via genomic alterations occur commonly in adult high-grade gliomas, and EGFR overexpression has been demonstrated in up to 85% of cases (Mellinghoff et al., 2005). Malignant gliomas also often exhibit overexpression of both platelet-derived growth factor (PDGF) and its receptor (PDGFR), which contribute to tumor progression via an autocrine or paracrine growth stimulation (Fleming et al., 1992). In addition, vascular endothelial growth factor (VEGF) and its receptor (VEGFR) contribute to the pathological angiogenesis seen in these tumors (Shinojima et al., 2003). The growth of glioma cells is also driven by constitutive activation of Akt, reflecting dysregulated receptor tyrosine kinase (RTK) signaling and loss of normal inhibitory mechanisms as a result of *PTEN* mutations (Abounader, 2009), which inhibits pro-apoptotic and cell cycle regulatory molecules.

RTK inhibitors induce glioma cell growth inhibition by blocking mitogenic signals through the Ras/Raf/MAPK pathway and anti-apoptotic signals through the PI3K/Akt pathway (Jane et al., 2006; Premkumar et al., 2006). However, previous studies using inhibitors targeted to a single RTK, such as EGFR or PDGFR, have yielded disappointing therapeutic results in malignant gliomas (Griffero et al., 2009), presumably reflecting that multiple compensatory signaling pathways can drive cell proliferation if a single pathway is blocked. This has focused attention toward evaluating multitargeted strategies for blocking multiple pathways in concert.

Vandetanib (ZACTIMA™) is an orally available anticancer agent that inhibits VEGFR, EGFR- and RET-dependent signaling (Carlomagno et al., 2002; Wedge et al., 2002; Ciardiello et al., 2003). In phase II studies in patients with advanced non-small-cell lung cancer (NSCLC), vandetanib had significant antitumor activity, both in monotherapy and

combination regimens (Heymach et al., 2008). Clinical trials of this agent in patients with malignant gliomas are currently in progress.

Histone deacetylase inhibitors (HDACIs) represent a class of agents that block the actions of histone deacetylases, which regulate gene expression by removal or addition of acetyl groups to core nucleosomal histones (Wolffe and Guschin, 2000). HDACIs promote histone acetylation, which favors a more open chromatin structure generally associated with enhanced transcription of a variety of genes, including the cell cycle regulators p21 and p27 (Marks et al., 2001). In this context, we have reported inhibition of cell proliferation and induction of apoptosis in glioma cells by trichostatin A (TSA), associated with increased $p21^{Cip/Waf}$ expression and decreased phosphorylated retinoblastoma protein (Rb) (Wetzel et al., 2005). Suberoylanalide hydroxamic acid (SAHA, vorinostat), an inhibitor of several members of the HDAC protein family (Finnin et al., 1999), has also been observed to have antiglioma activity in preclinical studies, causing GBM cells to accumulate in the G2-M phase of the cell cycle, with increased expression of p21WAF1 and p27KIP1, decreased levels of cyclin-dependent kinase (CDK) 2, CDK4, cyclin D1, and cyclin D2 (Yin et al., 2007), and inhibition of GBM growth in orthotopic models. Clinical trials testing combinations of HDACIs with other antineoplastic agents and irradiation have shown promising results (Al-Janadi et al., 2008).

Previous studies have shown that interruption of signaling pathways, including the MAPK and PI3K/Akt cascades, can lower the threshold for HDACI–induced cancer cell lethality (Nimmanapalli et al., 2003; Yu et al., 2003; Yu et al., 2005; Yu et al., 2007). Because vandetanib has been shown to inhibit EGFR, VEGFR-2, MAPK, and Akt activity, we hypothesized that combining vandetanib with HDACIs would lead to synergistic cytotoxicity in malignant human glioma cells. This study investigated the cytotoxic attributes of the combination of vandetanib with HDACIs in human glioma cells and the underlying molecular basis of the observed results. Our study shows that vandetanib synergistically potentiates HDACI–induced apoptosis by inactivating MAPK and Akt pathways. These

results suggest a potential strategy for increasing the clinical efficacy of RTK inhibitors in patients with gliomas and perhaps other malignancies.

Materials and Methods

Inhibitors and reagents.

Vandetanib was kindly provided by AstraZeneca (Macclesfield, UK). SAHA was purchased from Chemie Tek (Indianapolis, IN). TSA and sodium butyrate were purchased from Sigma (St. Louis, MO). Z-VAD-FMK was from Promega (Madison, WI). Human recombinant EGF was purchased from Cell Signaling Technology, Inc. (Beverly, MA); VEGF and PDGF from R&D Systems, Inc (Minneapolis, MN).

Cell culture.

The established malignant glioma cell lines U87, T98G, U373, and A172 were obtained from the American Type Culture Collection (Manassas, VA). Two other established glioma cell lines, LNZ308 and LNZ428, were generously provided by Dr. Nicolas de Tribolet. Human astrocytes were obtained from ScienCell Research Laboratories (San Diego, CA). U87, T98G, and U373 were cultured in growth medium composed of minimum essential medium supplemented with sodium pyruvate and nonessential amino acids; A172, LNZ308, and LNZ428 were cultured in α-minimal essential medium supplemented with L-glutamine; human astrocytes were cultured in astrocyte growth medium. All growth media contained 10% fetal calf serum, L-glutamine, 100 IU/ml penicillin, 100 mg/ml streptomycin, and 0.25 mg/ml amphotericin (Invitrogen, Carlsbad, CA).

These cell lines were chosen because they are widely available and exhibit a range of genomic alterations commonly seen in malignant gliomas, such as p53 mutations, *PTEN* deletions, and p16 deletions. Cells were grown in 75-cm^2 flasks at 37°C in a humidified atmosphere with 5% carbon dioxide and were subcultured every 4 to 7 days by treatment with 0.25% trypsin in Hanks' balanced salt solution (Invitrogen).

Cell proliferation and cytotoxicity assays.

Cells (5 x 10^3/well) were plated in 96-well microtiter plates (Costar, Cambridge, MA) in 100 µl of growth medium, and after overnight attachment, were exposed for 3 days to a range of concentrations of vandetanib and HDACIs, alone and in combination. Control cells received vehicle alone (DMSO). After the treatment interval, cells were washed in inhibitor-free medium, and the number of viable cells was determined using a colorimetric cell proliferation assay (CellTiter96 Aqueous NonRadioactive Cell Proliferation Assay; Promega), which measures the bioreduction of the tetrazolium compound 3-[4,5-dimethylthiazol-2yl]-5-[3-carboxymethoxyphenyl]-2-[4- sulfophenyl]-2*H* tetrazolium (MTS) by dehydrogenase enzymes of metabolically active cells into a soluble formazan product, in the presence of the electron coupling reagent phenazine methosulfate (Riss TL, 1992). All studies were conducted in triplicate and repeated at least three times independently. To perform the assay, 20 µl of MTS/phenazine methosulfate solution was added to each well, and after 1 h of incubation at 37°C in a humidified 5% CO_2 atmosphere, absorbance was measured at 490 nm in a microplate reader. Triplicate wells with predetermined cell numbers were subjected to the above-mentioned assay in parallel with the test samples to normalize the absorbance readings.

To assess cellular toxicity, 2.5 x 10^5 cells were seeded in 6-well dishes and on the following day, treated with selected concentrations of inhibitors or vehicle. Cells were harvested, stained with trypan blue, and counted using a hemacytometer. All samples were tested in triplicate. Viable (trypan blue-excluding) and dead cell numbers were plotted as a function of inhibitor concentration.

Clonogenic growth assay.

The effect of different inhibitor concentrations on cell viability was also assessed using a clonogenic assay. For this analysis, 250 cells were plated in six-well trays in growth medium, and after overnight attachment, cells were exposed to selected inhibitor concentrations or vehicle for 24 h. The cells were then washed with inhibitor-free medium

JPET Fast Forward. Published on July 21, 2009 as DOI: 10.1124/jpet.109.155705
This article has not been copyedited and formatted. The final version may differ from this version.

and allowed to grow for 2 weeks under inhibitor-free conditions. Colonies of a diameter of approximately 2 to 4 mm were counted directly. All studies were performed in triplicate.

Immunoprecipitation and Western blotting analysis.

Treated and untreated cells were washed in cold PBS and lysed in buffer containing 30 mM HEPES, 10% glycerol, 1% Triton X-100, 100 mM NaCl, 10 mM $MgCl_2$, 5 mM EDTA, 2mM Na_3VO4, 2 mM β-glycerophosphate, 1 mM phenylmethylsulfonyl fluoride, 1 mM 4-(2-aminoethyl)benzenesulfonyl fluoride, 0.8 μM aprotinin, 50 μM bestatin, 15 μM E-64, 20 μM leupeptin, and 10 μM pepstatin A for 15 min on ice. Samples were centrifuged at 12,000*g* for 15 min, supernatants were isolated, and protein was quantified using Protein Assay Reagent (Pierce Chemical, Rockford, IL). Equal amounts of protein were separated by SDS-polyacrylamide gel electrophoresis (PAGE) and electrotransferred onto a nylon membrane (Invitrogen). Nonspecific antibody binding was blocked by incubation of the blots with 2% bovine serum albumin in Tris-buffered saline (TBS)/Tween 20 (0.1%) for 1 h at room temperature. The blots were then probed with appropriate dilutions of primary antibody overnight at 4°C. The antibody-labeled blots were washed three times in TBS/Tween 20 for 15 min and then incubated with a 1:1500 dilution of horseradish peroxidase-conjugated secondary antibody (Santa Cruz Biotechnology, Inc.) in TBS/Tween 20 at room temperature for 1 h. After additional washing in TBS/Tween 20, the proteins were visualized by Western Blot Chemiluminescence Reagent (Cell Signaling Technology Inc., Beverly, MA). Where indicated, the blots were reprobed with antibodies against β-actin (Sigma- Aldrich, St. Louis, MO) to ensure equal loading and transfer of proteins. Primary antibodies to total EGFR and phospho-EGFR (Tyr845, Tyr1068, Tyr1086, Tyr1148, Tyr1173); total PDGFR-β and phospho-PDGFR-β (Tyr751); total VEGFR-2 and phospho-VEGFR-2 (Tyr1054/1059) were obtained from BioSource International (Camarillo, CA). Antibodies to cleaved caspase-3, cleaved PARP, Bax, ERK1/2 and phospho-p44/42 ERK (Thr202/Tyr204), Akt and phospho-Akt (Ser473), HSP90, acetyl-histone H2A, acetyl-histone H2B, acetyl-histone H3, acetyl-

histone H4, phospho-GSK-3β, p21 Cip/Waf, CDK4, CDK6, cyclin D1, and cyclin D3 were obtained from Cell Signaling Technology, Inc. (Beverly, MA).

For immunoprecipitation, cells were harvested in cell lysis buffer. The lysates were cleared of insoluble material by centrifugation at 12,000 x *g* for 15 min at 4 °C. Equal amounts of protein (300 μg) were incubated with 2 to 4 μg of anti-HSP90 antibody overnight at 4 °C and protein A-conjugated beads for another 3 h. Beads were washed three times with cell lysis buffer, and proteins were eluted with an SDS sample buffer for Western blotting analysis as described above.

Adenovirus infection.

PTEN wild-type adenovirus (Ad-PTEN-WT) was kindly provided by Dr. Craig Henke (University of Minnesota, Minneapolis, MN). Ad-myr-Akt adenovirus was purchased from Vector Biolabs (Eagleville, PA). A172 (PTEN deleted glioma cell line) cells were infected with adenovirus vectors at 100 multiplicity of infection (MOI). The cells were incubated for 36 h at 37 °C, the medium was changed and treated as indicated. Cells were lysed as described above and equal amount of protein was separated by PAGE and Western-blotted with the indicated antibodies.

Analysis of combinatorial effects.

Unless otherwise stated, data are expressed as mean ± S.D. The significance of differences between experimental conditions was determined using a two-tailed Student's *t* test. MTS assays were used to determine inhibition of cell survival after a 72 h treatment of multiple cell lines with different ratios of vandetanib and SAHA. IC_{50} concentrations and combination indices for the effects of vandetanib and SAHA were calculated using a commercially available software program (Calcusyn; Biosoft, Ferguson, MO) (Chou and Talalay, 1984).

JPET Fast Forward. Published on July 21, 2009 as DOI: 10.1124/jpet.109.155705
This article has not been copyedited and formatted. The final version may differ from this version.

Results

Vandetanib inhibits VEGFR-2, EGFR and PDGFR phosphorylation. Vandetanib has been reported to inhibit several receptor tyrosine kinases, including VEGFR, and EGFR (Ciardiello et al., 2003; Damiano et al., 2005). To confirm the specificity and dose-dependency of kinase inhibition, we examined the effect of vandetanib on several tyrosine kinase receptors that have been implicated in glioma growth. First we assessed the effect of vandetanib on the activation status of EGFR, including the phosphorylation of Tyr845, Tyr1068, Tyr1086, Tyr1148, and Tyr1173 with five different antibodies recognizing specific phosphorylation sites of EGFR (Fig. 1A). Treatment of T98G cells with concentrations of vandetanib as low as 2 μM produced nearly complete abrogation of EGFR tyrosine phosphorylation at Tyr845, and significant reduction of phosphorylation at the other sites examined (Fig. 1A). As shown in Figure 1B vandetanib was capable of inhibiting EGFR tyrosine kinase phosphorylation (Tyr845) in a dose-dependent manner in T98G and A172 glioma cell lines.

Next we examined the effect of vandetanib on EGF- and VEGF-mediated VEGFR-2 phosphorylation. T98G cells were pretreated with or without vandetanib for 2 h followed by 30 min of EGF or VEGF stimulation. Cell lysates were prepared and probed with antibodies recognizing phosphorylated VEGFR-2 monitored by Western blotting. EGF induced a marked increase in the activation of VEGFR-2 (Fig. 1C, lane 2). Interestingly EGF-induced VEGFR-2 activation was significantly reduced by vandetanib (Fig. 1C, lane 3) as was VEGF-induced phosphorylation (Fig. 1C, lane 4; and Fig. 1D). Consistent with the previously published results (Ciardiello et al., 2003), vandetanib was capable of inhibiting VEGFR-2 tyrosine kinase phosphorylation in a dose-dependent manner (Fig. 1D). Then to characterize the effects on PDGF-dependent receptor phosphorylation, T98G cells were treated with or without vandetanib followed by PDGF for 30 min. Compared with untreated control cells, PDGF (50 ng/ml) induced PDGFR phosphorylation (Fig. 1E, lane 6) and vandetanib reduced PDGF-induced receptor activation in a dose-dependent manner (Fig. 1F).

JPET Fast Forward. Published on July 21, 2009 as DOI: 10.1124/jpet.109.155705
This article has not been copyedited and formatted. The final version may differ from this version.

Vandetanib inhibits glioma cell proliferation and colony formation. To determine whether vandetanib could have a direct antiproliferative effect on glioma cell growth, six malignant human glioma cell lines were treated with different doses of vandetanib. Cells were cultured with increasing concentrations of vandetanib for 3 days and cell proliferation was assessed by MTS assay. Control cells were treated with equivalent concentrations of vehicle (DMSO) in the absence of vandetanib. As shown in Figure 2A, vandetanib treatment resulted in a dose-dependent inhibition of cell proliferation with IC_{50} values ranging between 7.2 and 18.5 μM. At these concentrations there were no significant effects on the normal cells such as human astrocytes (data not shown). The cytotoxic effect of vandetanib was further confirmed with a clonogenic assay (Figure 2B). Three different glioma cell lines were treated with varying concentrations of vandetanib for 1 day. Then the medium was aspirated, washed, and cells were allowed to grow for an additional 2-week period with inhibitor-free medium. There was a dose-dependent decrease in colony forming ability in response to treatment with vandetanib. As with the MTS studies, IC_{50} values for inhibition of clonogenicity were significantly higher than those noted for inhibition of phosphorylation of the primary receptor targets (Fig. 1).

Effect of vandetanib on EGFR downstream signaling pathways. To further identify the effect of vandetanib on EGFR downstream signaling that might contribute to the observed direct growth inhibition, we examined the phosphorylation of several key regulators involved. As shown in Figure 3, the phosphorylation of ERK/MAPK and Akt was significantly inhibited by vandetanib treatment in a dose-dependent manner in T98G cells, and to a lesser degree in U87 cells. Consistent with the inhibition of downstream signaling, phosphorylation of GSK-3β was completely abolished in T98G cells (data not shown). Vandetanib has previously been shown to cause G0/G1 cell cycle arrest in nasopharyngeal carcinoma cells, which was associated with an up-regulation of p21 and/or p27, and down-regulation of CDK4, CDK6 and CDK2 (Xiao et al., 2007). To understand the molecular mechanisms by which vandetanib inhibits proliferation of glioma cell lines, a number of key cell cycle regulatory proteins and pro-apoptotic molecules were examined. These include cyclins and their

JPET Fast Forward. Published on July 21, 2009 as DOI: 10.1124/jpet.109.155705
This article has not been copyedited and formatted. The final version may differ from this version.

catalytic partners, the CDKs. In T98G cells, vandetanib 25 μM resulted in a significant reduction in cyclin D1, and CDK4, paralleling the effects observed on Akt phosphorylation (Fig. 3B). Pro-apoptotic proteins were also examined by Western blotting analysis following treatment with varying concentrations of vandetanib for 24 h. As shown in Figure 3C, increases in the expression of cleaved Bax, cleaved caspase 3, and cleaved PARP were detected with vandetanib at a concentration of 25 μM (Fig. 3C).

Histone deacetylase inhibitors reduce cell proliferation of glioma cells in vitro. Because the concentrations of vandetanib required to inhibit cell proliferation, clonogenicity, and downstream signaling were noted to be above the clinically achievable range (Kiura et al., 2008), we questioned whether the activity of this agent could be enhanced by combination with other molecularly targeted agents that interfere with receptor-mediated signaling. Because previous studies have shown that inhibition of MAPK potentiates HDACI–induced apoptosis, and constitutive activation of MAPK protects against HDACI–induced cell death (Yu et al., 2005), we examined whether combination of vandetanib with HDAC inhibition might potentiate the effects of both agents and enhance the induction of apoptosis in malignant human glioma cell lines. We initially examined the independent effect of three different HDACIs, SAHA, TSA and sodium butyrate, on the proliferation of a panel of glioma cell lines using MTS assay. All three agents inhibited glioma cell proliferation in a dose-dependent manner (Fig. 4A, B and C). The cytotoxic effect of SAHA was further confirmed with a clonogenic assay (Fig. 4D). Four different glioma cell lines were treated with varying concentrations of SAHA for 1 day. Then the medium was aspirated, washed, and cells were allowed to grow for an additional 2-week period with inhibitor-free medium. There was a dose-dependent decrease in colony-forming ability in response to treatment with SAHA (Fig. 4D), although as with vandetanib, effective concentrations were at or above the maximal clinically achievable range.

Histone deacetylase inhibitors induce acetylated histones in glioma cells. To determine whether the in vitro responses to HDACIs correlated with changes in histone

acetylation, we assessed the effects of HDACIs on various HDAC-related biomarkers (histone H2A, H2B, H3 and H4 acetylation, and p21 expression) in three different glioma cell lines. Western blot analysis showed that exposure of glioma cells to HDACIs led to substantial increases in histone H2A, H2B, H3 and H4 acetylation (Fig. 5A). Time course analysis revealed that SAHA produced a robust histone H2A, H2B, H3 and H4 acetylation as early as 6 h at submicromolar concentrations (Fig. 5B). Because the CDK inhibitor p21WAF1 was increased in glioma cells by TSA (Wetzel et al., 2005), we tested the time course of SAHA-mediated p21 expression. Cells were exposed to varying concentrations of SAHA; lysates were prepared and probed with antibodies recognizing p21 Cip/Waf. Western blot analysis revealed that p21 expression lagged behind that of histone acetylation by at least 12 h (Fig. 5C).

Induction of enhanced cell death after exposure to vandetanib and HDACIs in glioma cells. The effect of combining vandetanib with HDACIs such as SAHA, TSA and sodium butyrate in T98G cells was then examined in relation to Bax and PARP cleavage. Whereas exposure to 2.0 μM vandetanib or HDACIs individually had modest or no effects on cleavage of caspase-3 and PARP, combined treatment resulted in a pronounced cleavage of these pro-apoptotic proteins (Fig. 6A). Induction in the levels of cleaved Bax (Fig. 6A) corresponded with increases in activated PARP levels in cells treated with a combination of both compounds, suggesting that treatment with a RTK inhibitor and HDACI combinations may be associated with activation of the intrinsic apoptosis pathway through activation of Bax. Consistent with these findings, combined treatment (but not treatment with vandetanib alone) resulted in a significant reduction in colony formation assessed by clonogenic assay ($p<0.001$; Fig. 6B). To formally examine the synergistic interaction in glioma cells, combination index studies were done for vandetanib (2 μM) combined with varying concentrations of SAHA (non-constant ratio). The combination resulted in a significant inhibition of cell proliferation (Fig. 7). To further examine the synergistic interaction, glioma cells were treated with varying concentrations of vandetanib and SAHA at a fixed ratio (1:10

constant ratio), and the combination index values for apoptosis induction were determined using the median effect method of Chou and Talalay (Chou and Talalay, 1984). As shown in Table 1, the combination index values were <1, indicating a synergistic interaction.

Effects of the combination of vandetanib and SAHA on signaling pathways. To elucidate the mechanistic basis for the synergistic cytotoxicity between vandetanib and SAHA, we determined the effects of this combination on various prosurvival signaling molecules in T98G, A172 and LNZ308 cells. In all three cell lines, combined treatment resulted in decreased phosphorylation of ERK1/2, at an early time point (6 h) (Fig. 8A, upper panel), when there was no significant induction of apoptosis as assessed by caspase 3 and PARP cleavage (data not shown). Combined exposure to vandetanib and SAHA also resulted in abrogation of ERK activation by 48 h (Fig. 8A, lower panel), leading to Bax and PARP cleavage (Fig. 6A). The total ERK levels remained unchanged with any treatment at 48 h.

Treatment with the novel HDACIs has been shown not only to induce acetylation of histones, p21, cell cycle growth arrest, and apoptosis but also to induce acetylation of HSP90. This is associated with polyubiquitylation, proteasomal degradation, and depletion of Akt, and c- Raf in chronic myeloid leukemia (CML) cells (Fuino et al., 2003; Nimmanapalli et al., 2003). Many proteins involved in the growth of malignant cells are associated with HSP90 (Young et al., 2001); disrupting this association targets the non-chaperoned proteins for degradation. To test whether the potentiating effects of SAHA on vandetanib efficacy reflected inhibition of Akt association with HSP90, T98G cells were exposed for 48 h to these agents alone or in combination, and cell lysates were collected. HSP90 protein was immunoprecipitated followed by immunoblotting with Akt. SAHA depleted Akt levels and co-treatment with SAHA and vandetanib completely abolished Akt association with HSP90, without significant effect on the levels of HSP90 itself (Fig. 8B).

We then tested the effects of vandetanib and SAHA combinations on the phosphorylation of Akt. T98G cells were treated with 2 μM SAHA or vandetanib alone or in

combination for 6 h or 48 h, and Western analysis was performed. In cells treated with the combination of vandetanib and SAHA, Akt phosphorylation was modestly reduced by the 6 h time point, and was completely abolished at the 48 h time point (Fig. 8C).

To better understand whether blockage of Erk1/2 and Akt cascades by vandetanib and SAHA-induced apoptosis, we used pharmacologic and genetic tools to perturb these pathways. First, A172 (PTEN deleted glioma cell line) cells were infected with Ad-CMV-PTEN or Ad-CMV-Myr-Akt. Thirty six hours after infection, cells were incubated with vandetanib or SAHA or combination of both for 48 h. Total proteins were then extracted for Western blot analysis and the percentage of apoptosis was determined by trypan blue exclusion assay. Cells infected with adenovirus expressing PTEN, which leads to Akt inhibition, or myristoylated Akt, which is constitutively active (Edinger and Thompson, 2002). Expression of wild-type PTEN, efficiently led to the dephosphorylation of Akt/PKB kinase (Fig. 8D), a downstream target of the PI-3 kinase–PTEN pathway that is dephosphorylated and inactivated by PTEN (Stambolic et al., 1998). Cells infected with Ad-myr-Akt exhibited a large increase in both the expression and phosphorylation of Akt, as expected (Fig. 8D, right). Treatment of these cells with vandetanib alone or in combination with SAHA modestly inhibited Akt phosphorylation, but there was still a large amount of phosphorylated Akt present even in the cells treated with the compound combinations. Treatment of cells infected with Ad-PTEN (WT) with this combination resulted in significant increase in PARP activation (Fig. 8D) and apoptosis (Fig. 8E). However, treatment of cells infected with Ad-myr-Akt with the compound combinations produced comparatively little effect on PARP cleavage (Fig. 8D) and apoptosis (Fig. 8E). Thus, we conclude that the synergism between vandetanib and SAHA in glioma cells is mediated, at least in part, via converging effects on Akt phosphorylation status and the consequences of this factor on downstream signaling.

To validate these results, T98G cells were exposed to vandetanib or SAHA in the presence or absence of pharmacologic inhibitors of MEK (U0126) and PI3K/Akt (LY294002). Cells were pretreated with U0126 or LY294002 in the complete media 60 min prior to treatment for 48 h. Total proteins were then extracted for Western blot analysis. Cells

treated with U0126 and LY294002 resulted in decreased phosphorylation of Erk1/2 and Akt respectively. Combined exposure to vandetanib and SAHA resulted in abrogation of ERK and Akt activation (Fig. 8F). As noted in Figure 6A, coadministration of vandetanib and SAHA resulted in activation of PARP. Inhibition of MEK/ERK and PI3K/Akt significantly enhanced vandetanib and SAHA-induced apoptosis in comparison with inhibition of either pathway (MEK or Akt) individually, suggesting that inactivation of MAPK and Akt play significant functional roles in the synergistic induction of apoptosis in malignant human glioma cells (Fig. 8D-F). To determine whether the observed cell death is indeed the consequence of caspase activation, we used the irreversible broad-range caspase inhibitor Z-VAD-FMK. Preincubation with the pan-caspase inhibitor Z-VAD-FMK rescued more than 30% of T98G cells from death induced by vandetanib and SAHA (Fig. 8G). Thus, cell death induced by vandetanib and SAHA was predominantly through caspase-dependent apoptosis.

Discussion

In the present study, we have evaluated the effects of the combination of a small molecule RTK inhibitor, vandetanib, which inhibited VEGFR-2, EGFR, and PDGFR tyrosine kinases, and SAHA, a HDAC inhibitor, in a panel of malignant human glioma cell lines. Our study demonstrated a significant synergistic anti-proliferative inhibition (combination index) according to the Chou and Talalay model for drug-drug interaction. This synergism in glioma cell growth inhibition appears to result from the efficient suppression of receptor phosphorylation and downstream MAPK and Akt pathway activation that are observed following combined treatment with these two classes of inhibitors. ERK/MAPK and Akt are each important effectors of EGFR signaling. In vandetanib-treated glioma cells, ERK/MAPK and Akt phosphorylation were inhibited in a dose-dependent manner, although the effects on Akt were comparatively modest, which may account for the limited effect on cell proliferation and apoptosis seen with clinically achievable concentrations of vandetanib alone. Akt is involved in cell cycle regulation by preventing GSK3β-mediated phosphorylation and

degradation of cyclin D1 (Cross et al., 1995) and by negatively regulating the CDK inhibitor p21 and p27 (Vivanco and Sawyers, 2002). Additionally, Akt has been shown to promote cell survival and suppress apoptosis via its ability to phosphorylate Bad (at Ser136) and subsequently liberate the Bcl-2 family (Kumar and Hung, 2005). Our results suggest that combined downregulation of ERK and Akt phosphorylation by vandetanib and SAHA may provide an effective strategy for inhibiting cell cycle progression and promoting apoptosis in glioma cells. This fits with other observations that combined downregulation of both Akt and ERK and elimination of compensatory interactions between these pathways may be considerably more therapeutically effective than interruption of either pathway alone (Shelton et al., 2004).

Our in vitro studies showed that HDACIs (SAHA, TSA and sodium butyrate) inhibited the growth of glioma cells in a dose-dependent and p53-independent manner. p53 mutant (T98G, U373), p53 deleted (LNZ308) and p53 wild-type (U87, A172) glioma cells were equally growth-inhibited by HDAC inhibitors. Other studies in glioma cells (Yin et al., 2007) as well as leukemic and breast cancer cells support a p53-independent inhibitory effect (Vrana et al., 1999; Huang et al., 2000). Although it has long been recognized that acetylation of histone proteins and resultant effects on regulation of chromatin structure and chromatin-directed activities such as transcription contribute to the therapeutic effects of HDACIs, it has become apparent in recent years that proteins other than histones are also regulated by acetylation and may be influenced by these agents. For example, HDAC inhibition results in acetylation of transcription factors that can modify their function (Peterson and Laniel, 2004), and of other key regulatory proteins, such as HSP90 (Bali et al., 2005), resulting in reduced association of HSP90 with its client proteins, such as EGFR, c-Src, STAT3, Akt, and other signaling intermediates necessary for survival (Edwards et al., 2007). Our results in T98G cells show that inhibition of HDAC function by SAHA results not only in increased acetylation of histones, but also decreased association of Akt with HSP90 (Fig. 8B), which is consistent with other recent observations that acetylation of chaperones such as HSP90 may lead to misfolding and degradation of client proteins (Edwards et al.,

2007), and may potentiate the effects seen with other HSP and proteasomal inhibitors (George et al., 2005).

Our observations suggest that the synergistic interactions between vandetanib and SAHA in glioma cells may reflect the combined effect of downregulating ERK1/2 by the former agent and downregulation/inactivation of the cytoprotective Akt pathway by the latter. The combined inactivation of ERK1/2 and Akt likely accounts for the significant potentiation of apoptosis induction in tumor cells exposed simultaneously to vandetanib and SAHA. This notion is consistent with previous findings that inactivation of ERK1/2 by the MEK inhibitor U0126 enhances HDAC-induced apoptosis (Yu et al., 2005). In agreement with other reports, we also noted that constitutive activation of Akt diminished the effect of combining an HDACI with a tyrosine kinase inhibitor (Yu et al., 2007). Conversely, constitutive inhibition of Akt activation by PTEN overexpression promoted the effects of these agents, alone and in combination.

Because numerous survival pathways are activated in transformed cells and form redundant signal transduction networks that interact with each other, it is likely that interruption of a single pathway will be insufficient to induce cell death or growth arrest, as other pathways may be able to compensate and promote tumor cell survival. An effective cancer therapy may well require interruption of multiple tumorigenic pathways in order to shift the balance of intracellular events toward death. Our results suggest that the downregulation of ERK/MAPK and Akt signaling by a combination of vandetanib and SAHA could be a potent approach to substantially enhance the antitumor effects of each agent alone, and warrants further preclinical and possible clinical evaluation.

Acknowledgment

We thank Naomi Agostino for her technical assistance.

References

Abounader R (2009) Interactions between PTEN and receptor tyrosine kinase pathways and their implications for glioma therapy. *Expert Rev Anticancer Ther* **9**:235-245.

Al-Janadi A, Chandana SR and Conley BA (2008) Histone deacetylation : an attractive target for cancer therapy? *Drugs R D* **9**:369-383.

Bali P, Pranpat M, Bradner J, Balasis M, Fiskus W, Guo F, Rocha K, Kumaraswamy S, Boyapalle S, Atadja P, Seto E and Bhalla K (2005) Inhibition of histone deacetylase 6 acetylates and disrupts the chaperone function of heat shock protein 90: a novel basis for antileukemia activity of histone deacetylase inhibitors. *J Biol Chem* **280**:26729-26734.

Carlomagno F, Vitagliano D, Guida T, Ciardiello F, Tortora G, Vecchio G, Ryan AJ, Fontanini G, Fusco A and Santoro M (2002) ZD6474, an orally available inhibitor of KDR tyrosine kinase activity, efficiently blocks oncogenic RET kinases. *Cancer Res* **62**:7284-7290.

Chou TC and Talalay P (1984) Quantitative analysis of dose-effect relationships: the combined effects of multiple drugs or enzyme inhibitors. *Adv Enzyme Regul* **22**:27-55.

Ciardiello F, Caputo R, Damiano V, Caputo R, Troiani T, Vitagliano D, Carlomagno F, Veneziani BM, Fontanini G, Bianco AR and Tortora G (2003) Antitumor effects of ZD6474, a small molecule vascular endothelial growth factor receptor tyrosine kinase inhibitor, with additional activity against epidermal growth factor receptor tyrosine kinase. *Clin Cancer Res* **9**:1546-1556.

Cross DA, Alessi DR, Cohen P, Andjelkovich M and Hemmings BA (1995) Inhibition of glycogen synthase kinase-3 by insulin mediated by protein kinase B. *Nature* **378**:785-789.

Damiano V, Melisi D, Bianco C, Raben D, Caputo R, Fontanini G, Bianco R, Ryan A, Bianco AR, De Placido S, Ciardiello F and Tortora G (2005) Cooperative antitumor effect of multitargeted kinase inhibitor ZD6474 and ionizing radiation in glioblastoma. *Clin Cancer Res* **11**:5639-5644.

Edinger AL and Thompson CB (2002) Akt maintains cell size and survival by increasing mTOR-dependent nutrient uptake. *Mol Biol Cell* **13**:2276-2288.

Edwards A, Li J, Atadja P, Bhalla K and Haura EB (2007) Effect of the histone deacetylase inhibitor LBH589 against epidermal growth factor receptor-dependent human lung cancer cells. *Mol Cancer Ther* **6**:2515-2524.

Finnin MS, Donigian JR, Cohen A, Richon VM, Rifkind RA, Marks PA, Breslow R and Pavletich NP (1999) Structures of a histone deacetylase homologue bound to the TSA and SAHA inhibitors. *Nature* **401**:188-193.

Fleming TP, Saxena A, Clark WC, Robertson JT, Oldfield EH, Aaronson SA and Ali IU (1992) Amplification and/or overexpression of platelet-derived growth factor receptors and epidermal growth factor receptor in human glial tumors. *Cancer Res* **52**:4550-4553.

Fuino L, Bali P, Wittmann S, Donapaty S, Guo F, Yamaguchi H, Wang HG, Atadja P and Bhalla K (2003) Histone deacetylase inhibitor LAQ824 down-regulates Her-2 and

sensitizes human breast cancer cells to trastuzumab, taxotere, gemcitabine, and epothilone B. *Mol Cancer Ther* **2**:971-984.

George P, Bali P, Annavarapu S, Scuto A, Fiskus W, Guo F, Sigua C, Sondarva G, Moscinski L, Atadja P and Bhalla K (2005) Combination of the histone deacetylase inhibitor LBH589 and the hsp90 inhibitor 17-AAG is highly active against human CML-BC cells and AML cells with activating mutation of FLT-3. *Blood* **105**:1768-1776.

Griffero F, Daga A, Marubbi D, Capra MC, Melotti A, Pattarozzi A, Gatti M, Bajetto A, Porcile C, Barbieri F, Favoni RE, Lo Casto M, Zona G, Spaziante R, Florio T and Corte G (2009) Different Response of Human Glioma Tumor-initiating Cells to Epidermal Growth Factor Receptor Kinase Inhibitors. *J Biol Chem* **284**:7138-7148.

Heymach JV, Paz-Ares L, De Braud F, Sebastian M, Stewart DJ, Eberhardt WE, Ranade AA, Cohen G, Trigo JM, Sandler AB, Bonomi PD, Herbst RS, Krebs AD, Vasselli J and Johnson BE (2008) Randomized phase II study of vandetanib alone or with paclitaxel and carboplatin as first-line treatment for advanced non-small-cell lung cancer. *J Clin Oncol* **26**:5407-5415.

Huang L, Sowa Y, Sakai T and Pardee AB (2000) Activation of the p21WAF1/CIP1 promoter independent of p53 by the histone deacetylase inhibitor suberoylanilide hydroxamic acid (SAHA) through the Sp1 sites. *Oncogene* **19**:5712-5719.

Jane EP, Premkumar DR and Pollack IF (2006) Coadministration of sorafenib with rottlerin potently inhibits cell proliferation and migration in human malignant glioma cells. *J Pharmacol Exp Ther* **319**:1070-1080.

Kiura K, Nakagawa K, Shinkai T, Eguchi K, Ohe Y, Yamamoto N, Tsuboi M, Yokota S, Seto T, Jiang H, Nishio K, Saijo N and Fukuoka M (2008) A randomized, double-blind, phase IIa dose-finding study of Vandetanib (ZD6474) in Japanese patients with non-small cell lung cancer. *J Thorac Oncol* **3**:386-393.

Kumar R and Hung MC (2005) Signaling intricacies take center stage in cancer cells. *Cancer Res* **65**:2511-2515.

Marks P, Rifkind RA, Richon VM, Breslow R, Miller T and Kelly WK (2001) Histone deacetylases and cancer: causes and therapies. *Nat Rev Cancer* **1**:194-202.

Mellinghoff IK, Wang MY, Vivanco I, Haas-Kogan DA, Zhu S, Dia EQ, Lu KV, Yoshimoto K, Huang JH, Chute DJ, Riggs BL, Horvath S, Liau LM, Cavenee WK, Rao PN, Beroukhim R, Peck TC, Lee JC, Sellers WR, Stokoe D, Prados M, Cloughesy TF, Sawyers CL and Mischel PS (2005) Molecular determinants of the response of glioblastomas to EGFR kinase inhibitors. *N Engl J Med* **353**:2012-2024.

Nimmanapalli R, Fuino L, Bali P, Gasparetto M, Glozak M, Tao J, Moscinski L, Smith C, Wu J, Jove R, Atadja P and Bhalla K (2003) Histone deacetylase inhibitor LAQ824 both lowers expression and promotes proteasomal degradation of Bcr-Abl and induces apoptosis of imatinib mesylate-sensitive or -refractory chronic myelogenous leukemia-blast crisis cells. *Cancer Res* **63**:5126-5135.

Peterson CL and Laniel MA (2004) Histones and histone modifications. *Curr Biol* **14**:R546-551.

Premkumar DR, Arnold B and Pollack IF (2006) Cooperative inhibitory effect of ZD1839 (Iressa) in combination with 17-AAG on glioma cell growth. *Mol Carcinog* **45**:288-301.

Riss TL MR (1992) Comparison of MTT, XTT and a novel tetrazolium compound MTS for in vitro proliferation and chemosensitivity assays. *Mol Biol Cell* **3**:184.

Shelton JG, Blalock WL, White ER, Steelman LS and McCubrey JA (2004) Ability of the activated PI3K/Akt oncoproteins to synergize with MEK1 and induce cell cycle progression and abrogate the cytokine-dependence of hematopoietic cells. *Cell Cycle* **3**:503-512.

Shinojima N, Tada K, Shiraishi S, Kamiryo T, Kochi M, Nakamura H, Makino K, Saya H, Hirano H, Kuratsu J, Oka K, Ishimaru Y and Ushio Y (2003) Prognostic value of epidermal growth factor receptor in patients with glioblastoma multiforme. *Cancer Res* **63**:6962-6970.

Stambolic V, Suzuki A, de la Pompa JL, Brothers GM, Mirtsos C, Sasaki T, Ruland J, Penninger JM, Siderovski DP and Mak TW (1998) Negative regulation of PKB/Akt-dependent cell survival by the tumor suppressor PTEN. *Cell* **95**:29-39.

Vivanco I and Sawyers CL (2002) The phosphatidylinositol 3-Kinase AKT pathway in human cancer. *Nat Rev Cancer* **2**:489-501.

Vrana JA, Decker RH, Johnson CR, Wang Z, Jarvis WD, Richon VM, Ehinger M, Fisher PB and Grant S (1999) Induction of apoptosis in U937 human leukemia cells by suberoylanilide hydroxamic acid (SAHA) proceeds through pathways that are regulated by Bcl-2/Bcl-XL, c-Jun, and p21CIP1, but independent of p53. *Oncogene* **18**:7016-7025.

Wedge SR, Ogilvie DJ, Dukes M, Kendrew J, Chester R, Jackson JA, Boffey SJ, Valentine PJ, Curwen JO, Musgrove HL, Graham GA, Hughes GD, Thomas AP, Stokes ES,

Curry B, Richmond GH, Wadsworth PF, Bigley AL and Hennequin LF (2002) ZD6474 inhibits vascular endothelial growth factor signaling, angiogenesis, and tumor growth following oral administration. *Cancer Res* **62**:4645-4655.

Wetzel M, Premkumar DR, Arnold B and Pollack IF (2005) Effect of trichostatin A, a histone deacetylase inhibitor, on glioma proliferation in vitro by inducing cell cycle arrest and apoptosis. *J Neurosurg* **103**:549-556.

Wolffe AP and Guschin D (2000) Review: chromatin structural features and targets that regulate transcription. *J Struct Biol* **129**:102-122.

Xiao X, Wu J, Zhu X, Zhao P, Zhou J, Liu QQ, Zheng L, Zeng M, Liu R and Huang W (2007) Induction of cell cycle arrest and apoptosis in human nasopharyngeal carcinoma cells by ZD6474, an inhibitor of VEGFR tyrosine kinase with additional activity against EGFR tyrosine kinase. *Int J Cancer* **121**:2095-2104.

Yin D, Ong JM, Hu J, Desmond JC, Kawamata N, Konda BM, Black KL and Koeffler HP (2007) Suberoylanilide hydroxamic acid, a histone deacetylase inhibitor: effects on gene expression and growth of glioma cells in vitro and in vivo. *Clin Cancer Res* **13**:1045-1052.

Young JC, Moarefi I and Hartl FU (2001) Hsp90: a specialized but essential protein-folding tool. *J Cell Biol* **154**:267-273.

Yu C, Dasmahapatra G, Dent P and Grant S (2005) Synergistic interactions between MEK1/2 and histone deacetylase inhibitors in BCR/ABL+ human leukemia cells. *Leukemia* **19**:1579-1589.

Yu C, Friday BB, Lai JP, McCollum A, Atadja P, Roberts LR and Adjei AA (2007) Abrogation of MAPK and Akt signaling by AEE788 synergistically potentiates histone deacetylase inhibitor-induced apoptosis through reactive oxygen species generation. *Clin Cancer Res* **13**:1140-1148.

Yu C, Rahmani M, Almenara J, Subler M, Krystal G, Conrad D, Varticovski L, Dent P and Grant S (2003) Histone deacetylase inhibitors promote STI571-mediated apoptosis in STI571-sensitive and -resistant Bcr/Abl+ human myeloid leukemia cells. *Cancer Res* **63**:2118-2126.

JPET Fast Forward. Published on July 21, 2009 as DOI: 10.1124/jpet.109.155705
This article has not been copyedited and formatted. The final version may differ from this version.

This work was supported by National Institutes of Health Grant [P01NS40923].

[§]ZACTIMA is a registered trademark of the AstraZeneca group of companies.

JPET Fast Forward. Published on July 21, 2009 as DOI: 10.1124/jpet.109.155705
This article has not been copyedited and formatted. The final version may differ from this version.

Figure Legends

Figure 1. Effects of vandetanib on receptor phosphorylation. **A**. T98G cells were seeded at 60% confluence and allowed to attach. Then, the cells were serum-starved 24 h and pretreated with 2 μM vandetanib for 2 h and then left untreated or treated with 50 ng/ml EGF for 30 min. Cell extracts were prepared, and equal amounts of protein (30 μg/ lane) were separated by SDS-PAGE analysis and subjected to Western blotting analysis with the indicated primary antibodies. **B**. T98G and A172 cells were seeded at sub-confluence and incubated overnight at 37^{o}C. Then, the cells were serum-starved for 24 h and pretreated with 0 to 2 μM vandetanib for 2 h and then left untreated or treated with 50 ng/ml EGF. Cell extracts were prepared, and equal amounts of protein were separated and subjected to Western blotting analysis with phospho-EGFR antibody (Tyr845). The blots were subsequently stripped and reprobed against total EGFR. **C.** T98G cells were seeded as mentioned above. After 24 h serum-starvation, cells were pretreated with 2 μM vandetanib for 2 h and then left untreated or treated with 50 ng/ml EGF or 50 ng/ml VEGF for 30 min. Western blotting was carried out as described in “Materials and Methods” and probed with indicated antibodies. **D**. After overnight attachment, T98G cells were serum-starved for 24 h and pretreated with 0 to 2 μM vandetanib for 2 h and then left untreated or treated with 50 ng/ml VEGF. Cell extracts were prepared, and equal amounts of protein were separated and subjected to Western blotting analysis with phospho-VEGFR-2 antibody. The blots were subsequently stripped and reprobed against total VEGFR-2. **E.** T98G cells were serum-starved for 24 h and pretreated with 2 μM vandetanib for 2 h and then left untreated or treated with 50 ng/ml EGF, 50 ng/ml VEGF, and 50 ng/ml PDGF for 30 min. Cell extracts were prepared, and equal amounts of protein (30 μg/ lane) were separated by SDS-PAGE analysis and subjected to Western blotting analysis with the phospho-PDGFRβ antibody. Subsequently, the blot was stripped and reprobed with total PDGFRβ antibody. **F**. T98G cells were seeded at sub-confluence and incubated overnight at 37^{o}C. Then, the cells were serum-starved for 24 h and pretreated with 0- to 2 μM vandetanib for 2 h and then left

untreated or treated with 50 ng/ml PDGF. Cell extracts were prepared, and equal amounts of protein were separated and subjected to Western blotting analysis with phospho-PDGFRβ antibody. The blots were subsequently stripped and reprobed against total PDGFRβ.

Figure 2. Effects of vandetanib on cellular proliferation and colony formation. **A**. Logarithmically growing established human glioma cell lines were incubated with varying concentrations of vandetanib for 3 days. The relationship between vandetanib and cell numbers was assessed semiquantitatively by spectrophotometric measurement of MTS bioreduction in six established malignant human glioma cell lines. Points represent the mean of four measurements ± S.D. There was a dose-dependent reduction in cell growth. Control cells were treated with equivalent concentrations of vehicle (DMSO). **B**. Graph showing the relationship between colony counts (± standard deviation) and concentration of the inhibitors. Human glioma cell lines U87, A172 and T98G were exposed to the indicated concentrations of vandetanib for 24 h. On the following day, the media was changed and complete media was added. Cells were grown for an additional 14 days in the absence of inhibitors. Control cells (0) were treated with equivalent concentrations of vehicle (DMSO). Colonies were then counted. Points represent the mean of two experiments ± standard deviation.

Figure 3. Effects of vandetanib on cell survival and cell cycle regulatory proteins. **A.** Logarithmically growing U87 and T98G cells were incubated with varying concentrations of vandetanib for 24 h. The cells were lysed, and equal amounts of proteins were separated by SDS-PAGE and probed with specific antibodies against phospho-ERK, and phospho-Akt. Western analysis was performed as described under Materials and Methods. The blots were subsequently stripped and reprobed against total ERK, Akt or β-actin. **B**. Logarithmically growing T98G cells were incubated with varying concentrations of vandetanib for 24 h. The cells were lysed, and equal amounts of proteins were separated by SDS-PAGE and probed with indicated cell cycle regulatory antibodies. **C**. T98G cells were incubated with varying

concentrations of vandetanib for 24 h. The cells were lysed, and equal amounts of proteins were separated by SDS-PAGE and probed with antibodies recognizing proapoptotic proteins. Western analysis was performed as described under Materials and Methods.

Figure 4. Effects of HDAC inhibitors on cellular proliferation and colony formation. Logarithmically growing established human glioma cell lines were incubated with varying concentrations of SAHA (**A**), Trichostatin A (**B**), or sodium butyrate (**C**) for 3 days. The relationship between vandetanib concentration and cell numbers was assessed semiquantitatively by spectrophotometric measurement of MTS bioreduction in six established malignant human glioma cell lines. Points represent the mean of four measurements ± S.D. There was a dose-dependent reduction in cell growth. Control cells were treated with equivalent concentrations of vehicle (DMSO). **D**. Graph showing the relationship between colony counts (± standard deviation) and SAHA concentration. Human glioma cell lines U87, A172, LNZ308 and T98G were exposed to the indicated concentrations of SAHA for 24 h. On the following day, the media was changed, complete media was added and cells were grown for an additional 14 days in the absence of inhibitors. Control cells (0) were treated with equivalent concentrations of vehicle (DMSO). Colonies were then counted. Points represent the mean of two experiments ± standard deviation.

Figure 5. Effects of HDAC inhibitors on histone acetylation and p21 expression. Logarithmically growing T98G, A172, and LNZ308 cell lines were incubated for 24 h in the presence of 2 μM SAHA, 250 nM trichostatin A (TSA), or 2.5 mM sodium butyrate (NaBt). The cells were lysed, and proteins were separated by SDS-PAGE and probed with specific antibodies. Western analysis was performed as described in ‘‘Materials and Methods.’’. The blots were subsequently stripped and reprobed with antibodies directed against ß-actin (**A**). Logarithmically growing T98G cell lines were incubated for designated intervals in the presence of 2 μM SAHA. The cells were lysed, and proteins were separated by SDS-PAGE

and probed with specific antibodies. The blots were subsequently stripped and reprobed with antibodies directed against ß-actin (**B**). T98G cells were incubated for designated intervals in the presence of 2 μM SAHA. The cells were lysed, and proteins were separated by SDS-PAGE and probed with specific antibodies against p21 Cip/Waf (**C**). Western analysis was performed as described in 'Materials and Methods'.

Figure 6. Effects of HDAC inhibitors and vandetanib on caspase-3 and Bax activation and colony formation in glioma cells. **A**. Logarithmically growing T98G cells were incubated for 48 h in the presence of 2 μM SAHA, 250 nM trichostatin A (TSA), or 2.5 mM sodium butyrate with or without vandetanib (2 μM). The cells were lysed, and proteins were separated by SDS-PAGE and probed with specific antibodies. Western analysis was performed as described in ''Materials and Methods.''. The blots were subsequently stripped and reprobed with antibodies directed against ß-actin. **B**. Graph showing the relationship between colony counts (± standard deviation) and concentration of the inhibitors. Human glioma cell lines T98G were exposed to indicated concentrations of SAHA with or without 2 μM vandetanib for 24 h. On the following day, the media was changed and complete media was added and cells were grown for additional 14 d in the absence of inhibitors. Control cells (0) were treated with equivalent concentrations of vehicle (DMSO). Colonies were then counted. Points represent the mean of two experiments ± standard deviation. **, $P<0.001$ versus vandetanib alone.

Fig. 7. Vandetanib enhances SAHA-induced cell proliferation inhibition. (A) Logarithmically growing glioma cell lines were incubated with or without varying concentrations of SAHA with or without 2 μM vandetanib for 3 days. The relationship between SAHA concentration and cell numbers was assessed semiquantitatively by spectrophotometric measurement of MTS bioreduction in T98G, U373, A172, and LNZ428, established malignant human glioma cell lines. Points represent the mean of three measurements ± standard deviation. There was a dose-dependent reduction in cell growth

and addition of 2 μM vandetanib potentiated the SAHA-induced toxicity. No significant inhibition was detected in control cells treated with equivalent concentrations of vehicle (DMSO) or 2 μM vandetanib alone (see Figure 2A for vandetanib dose response).

Fig. 8. Combination of vandetanib and SAHA modulates survival and other regulatory molecules. A. Logarithmically growing T98G, A172 and LNZ308 cell lines were incubated in the presence of 2μM SAHA with or without vandetanib (2 μM) for different durations. Cells were lysed and 30 μg of total protein/lane was separated by SDS-PAGE and subjected to immunoblot analysis with phospho ERK 1/2 antibodies. Western analysis was performed as described under Materials and Methods. The blots were subsequently stripped and reprobed against total ERK. **B.** T98G cells were incubated in the presence of 2μM SAHA with or without vandetanib (2 μM) for 48 h, after which HSP90 was immunoprecipitated (IP) from the cell lysates and immunoblotted (WB) with either anti-HSP90 or total Akt. Immunoprecipitation and Western analysis was performed as described in Materials and Methods. **C**. Logarithmically growing T98G cells were incubated in the presence of 2μM SAHA with or without vandetanib (2 μM) for the indicated durations. Cells were lysed and 30 μg of total protein/lane was separated by SDS-PAGE and subjected to immunoblot analysis with the phospho Akt (Ser 473) antibody. Western analysis was performed as described under Materials and Methods. The blots were subsequently stripped and reprobed against total Akt. **D**. Logarithmically growing A172 cells were infected with wild-type PTEN or constitutively active form of Akt (Ad-myr-Akt) at 100 MOI per cell. Thirty-six hours after infection, cells were incubated in the presence of SAHA (2μM) with or without vandetanib (2 μM) for 48 h. Control cells received DMSO. Cells were lysed and 30 μg of total protein/lane was separated by SDS-PAGE and subjected to immunoblot analysis with the indicated antibodies. **E.** Logarithmically growing A172 cells were infected with wild-type PTEN (Ad-PTEN) or constitutively active form of Akt (Ad-myr-Akt) at 100 MOI per cell. Thirty-six hours after infection, cells were incubated in the presence of SAHA (2μM) and vandetanib (2 μM) for 48 h. Control cells received DMSO. At the end of the incubation

period, the viable cell numbers were determined by trypan-blue exclusion assay. For each analysis, at least 400 cells were evaluated in duplicate. The values represent the mean ± standard deviation for two separate experiments performed in triplicate (**, P<0.005). **F.** Logarithmically growing T98G cells were exposed to vandetanib (2μM) or SAHA (2μM) or the combination of both with or without U0126 or LY294002. Cells were pretreated with U0126 (5 μM) or LY294002 (5 μM) in the complete media 60 min prior to treatment with vandetanib and/or SAHA for 48 h. Western immunoblot analysis was performed with the indicated antibodies. **G.** T98G cells were pretreated with or without 50 μM Z-VAD-FMK (ZVS) in the complete media 60 min prior to treatment with vandetanib (2μM) and SAHA (2μM) (VS) for 48 h. Control cells received DMSO (C). At the end of the incubation period, the viable cell numbers were determined by trypan-blue exclusion assay. For each analysis, at least 400 cells were evaluated in duplicate. The values represent the mean ± standard deviation for two separate experiments performed in triplicate (**, P<0.001).

JPET Fast Forward. Published on July 21, 2009 as DOI: 10.1124/jpet.109.155705
This article has not been copyedited and formatted. The final version may differ from this version.

Table 1.

Combination Index (CI) at IC50 in malignant glioma cells

Cell line	CI
U87	0.465 ± 0.039
T98G	0.614 ± 0.041
A172	0.621 ± 0.028
U373	0.407 ± 0.011
LNZ308	0.421 ± 0.031
LNZ428	0.443 ± 0.024

Six established human glioma cell lines were exposed to varying concentrations of SAHA and vandetanib at a fixed molar ratio (1:10) for 3 days. Live cell numbers at the end of treatment were quantified with MTS reagents. The data were then used to calculate the combination index (CI) using commercially available software (Calcusyn; Biosoft), which provides a semiquantitative assessment of the presence of additive, synergistic, or antagonistic interactions at different effect levels. The CI is substantially less than 1 for the combination of SAHA and vandetanib, indicating synergistic interactions. Data are the average of three independent experiments with triplicate samples.

Fig.1

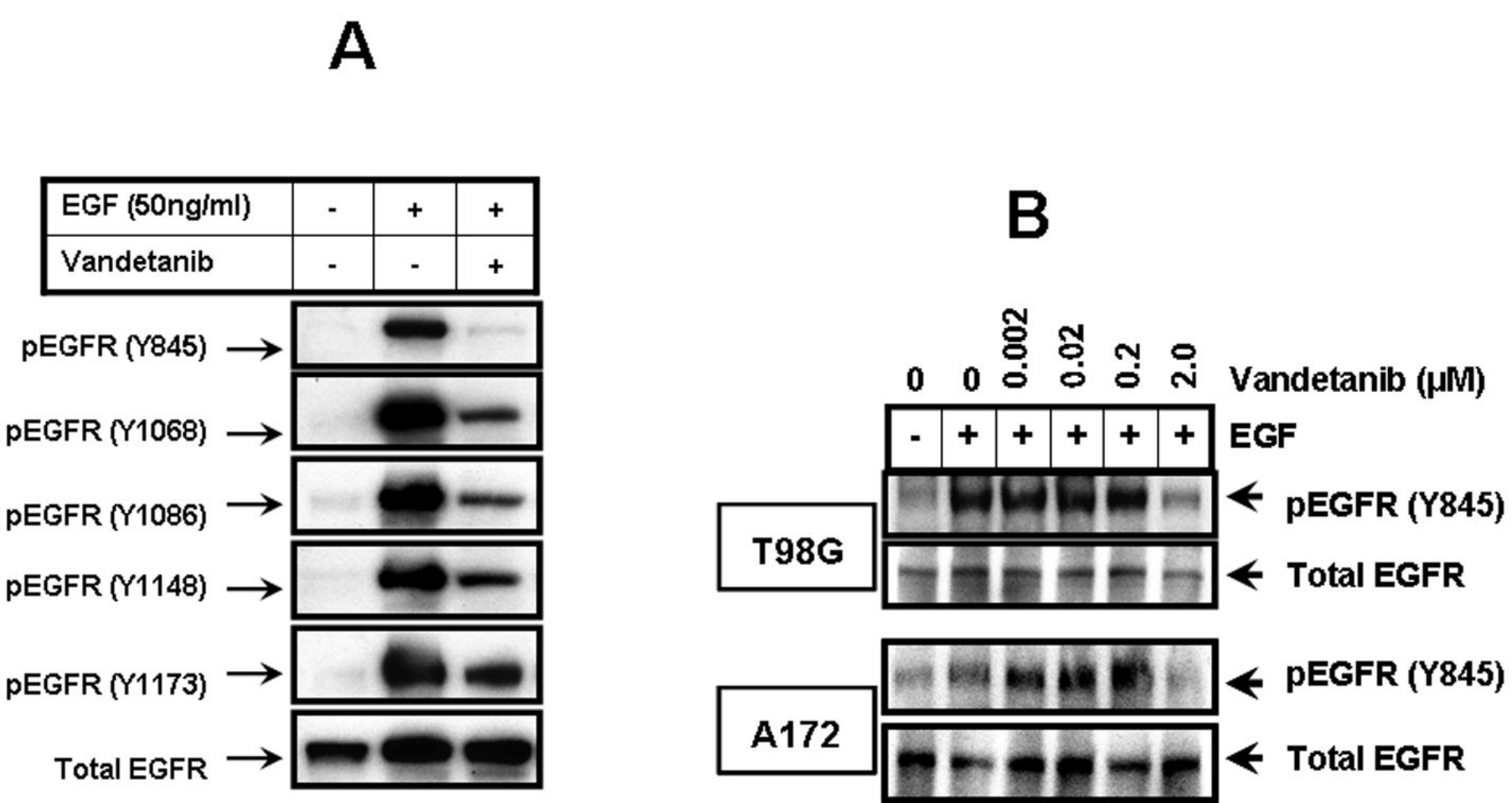
A
EGF (50ng/ml) - + +
Vandetanib - - +
pEGFR (Y845)
pEGFR (Y1068)
pEGFR (Y1086)
pEGFR (Y1148)
pEGFR (Y1173)
Total EGFR
B
0 0 0.002 0.02 0.2 2.0 Vandetanib (μM)
- + + + + + EGF
T98G
pEGFR (Y845)
Total EGFR
A172
pEGFR (Y845)
Total EGFR

Fig.1

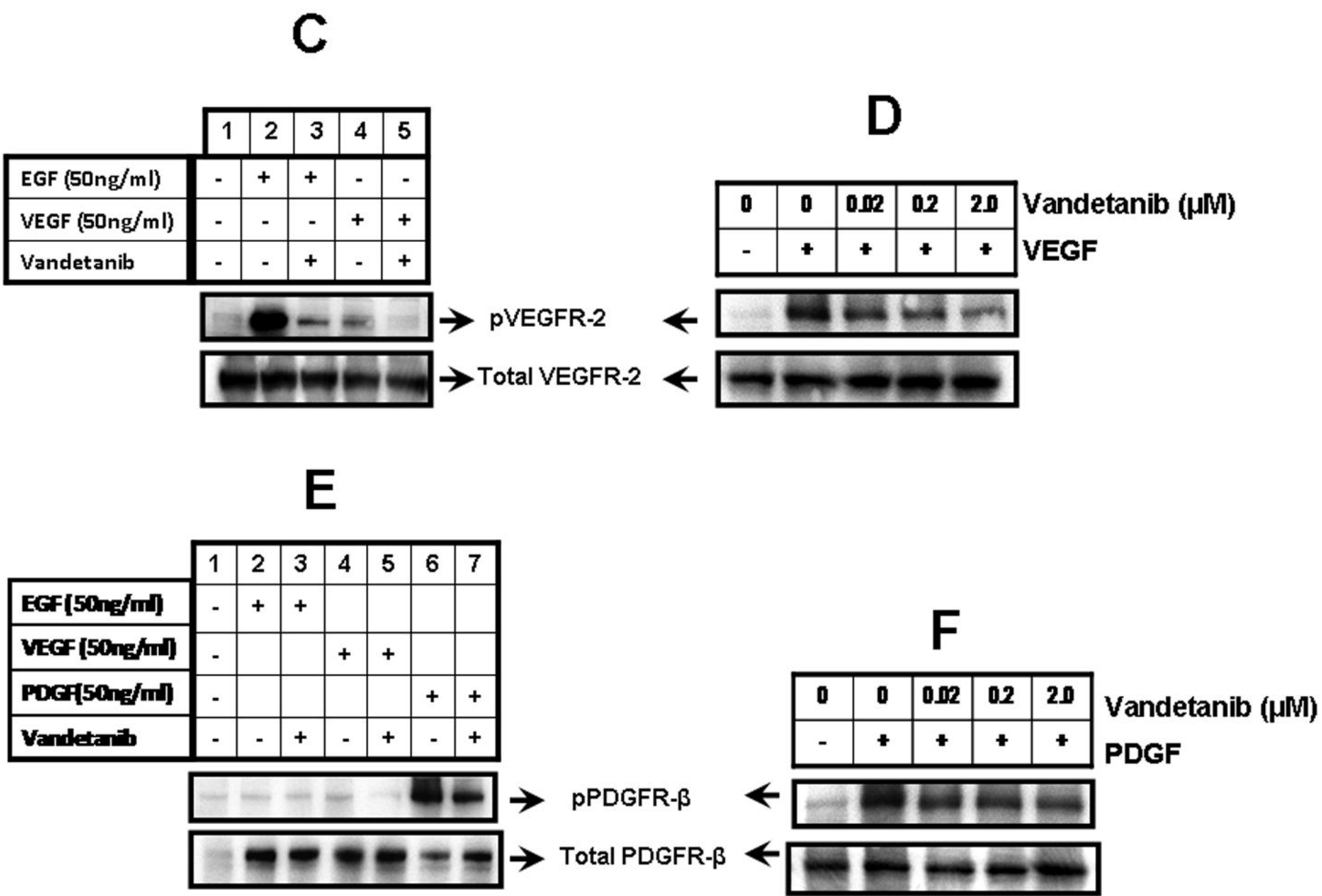
C
1 2 3 4 5
EGF (50ng/ml) - + + - -
VEGF (50ng/ml) - - - + +
Vandetanib - - + - +
pVEGFR-2
Total VEGFR-2
D
0 0 0.02 0.2 2.0 Vandetanib (μM)
- + + + + VEGF
E
1 2 3 4 5 6 7
EGF (50ng/ml) - + +
VEGF (50ng/ml) - + +
PDGF(50ng/ml) - + +
Vandetanib - - + - + - +
pPDGFR-β
Total PDGFR-β
F
0 0 0.02 0.2 2.0 Vandetanib (μM)
- + + + + PDGF

Fig.2

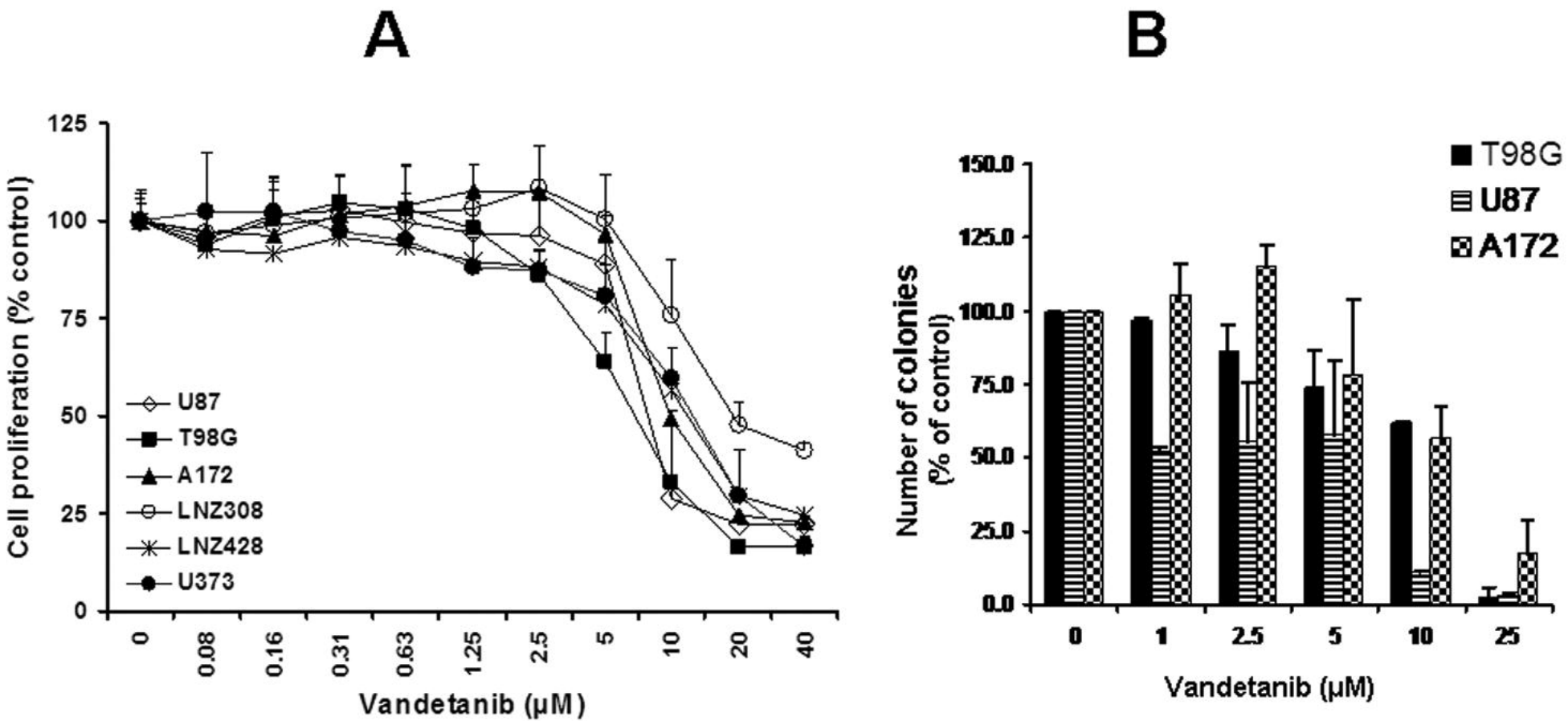
A
Cell proliferation (% control)
125
100
75
50
25
0
U87
T98G
A172
LNZ308
LNZ428
U373
0
0.08
0.16
0.31
0.63
1.25
2.5
5
10
20
40
Vandetanib (μM)
B
Number of colonies (% of control)
150.0
125.0
100.0
75.0
50.0
25.0
0.0
T98G
U87
A172
0
1
2.5
5
10
25
Vandetanib (μM)

Fig.3

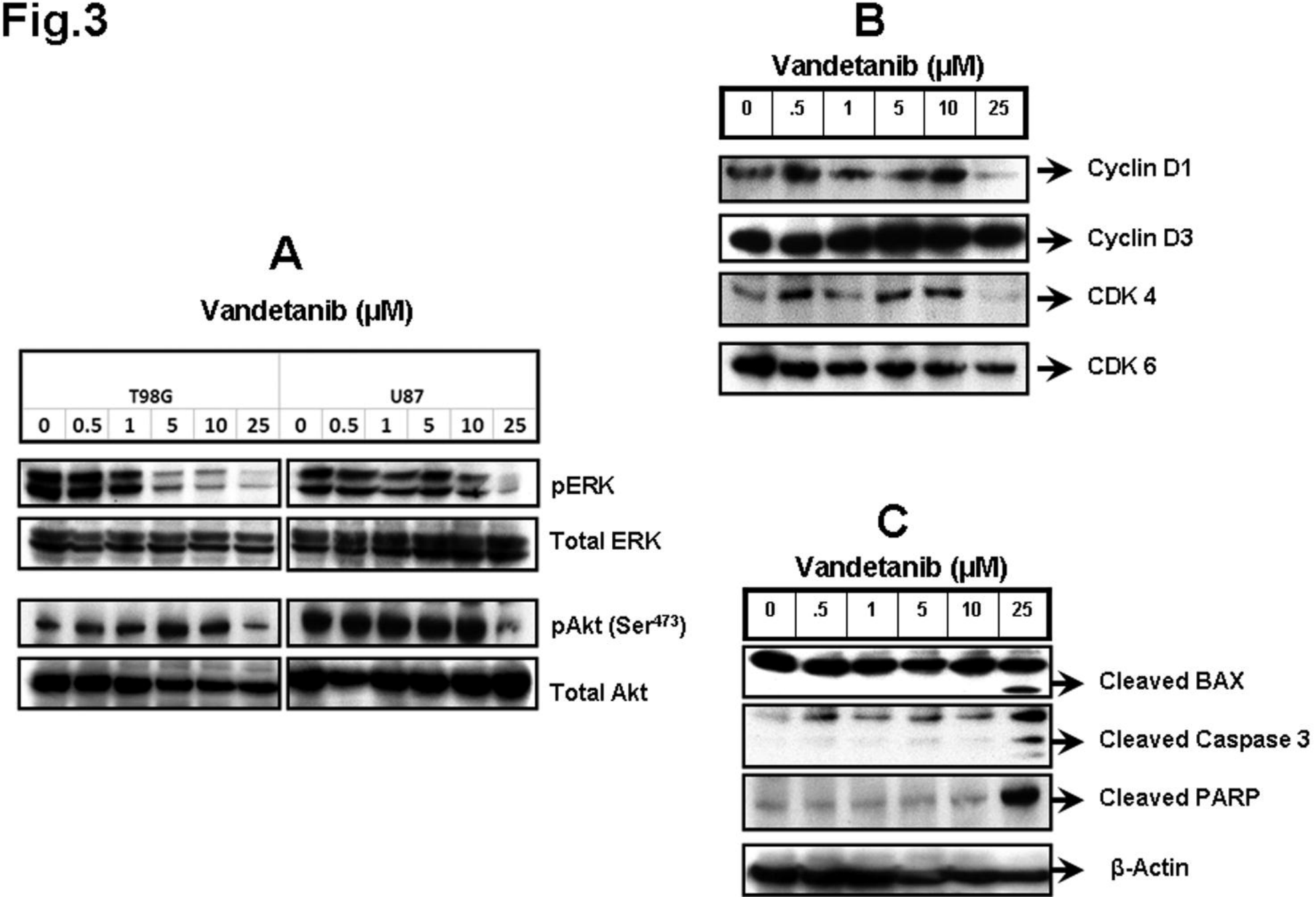
A
Vandetanib (μM)
T98G
U87
0 0.5 1 5 10 25 0 0.5 1 5 10 25
pERK
Total ERK
pAkt (Ser473)
Total Akt
B
Vandetanib (μM)
0 .5 1 5 10 25
Cyclin D1
Cyclin D3
CDK 4
CDK 6
C
Vandetanib (μM)
0 .5 1 5 10 25
Cleaved BAX
Cleaved Caspase 3
Cleaved PARP
β-Actin

Fig.4

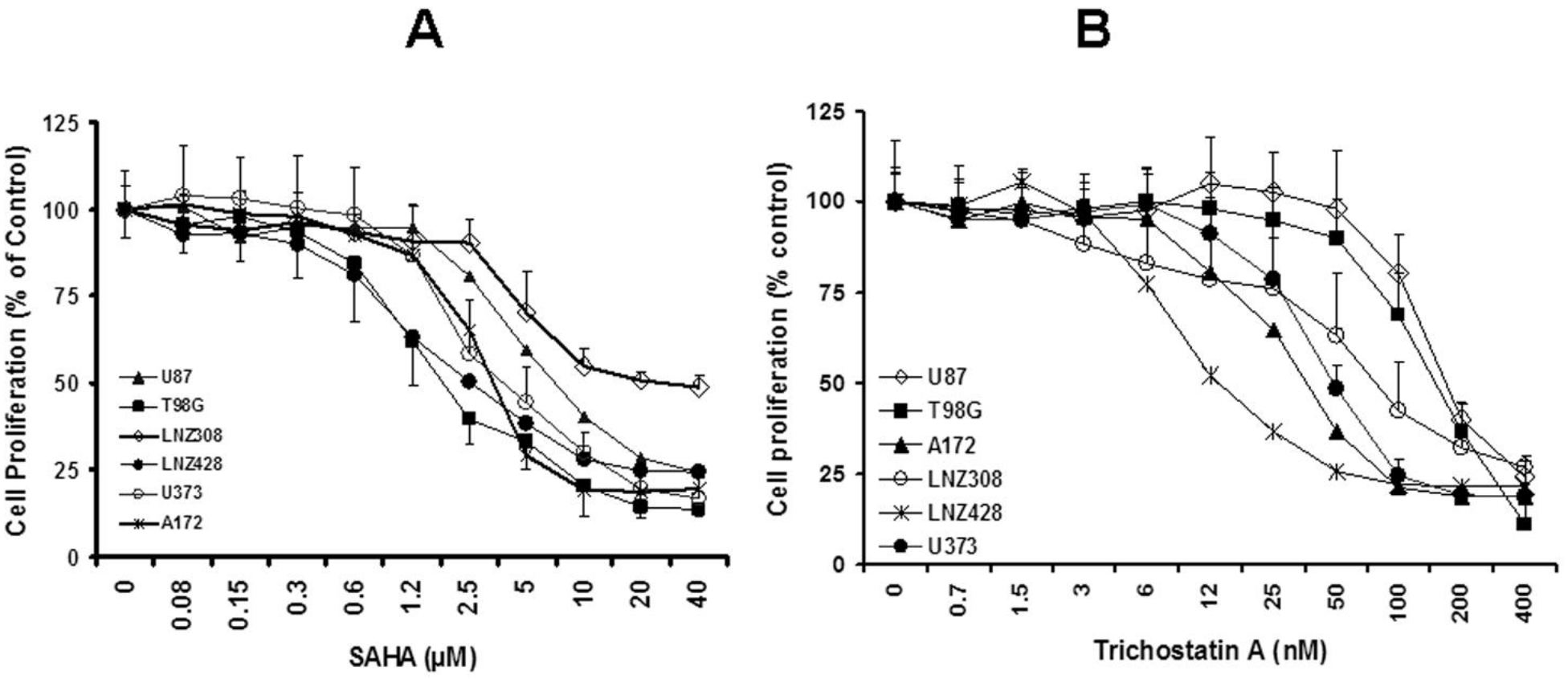
A
Cell Proliferation (% of Control)
125
100
75
50
25
0
U87
T98G
LNZ308
LNZ428
U373
A172
0
0.08
0.15
0.3
0.6
1.2
2.5
5
10
20
40
SAHA (μM)
B
Cell proliferation (% control)
125
100
75
50
25
0
U87
T98G
A172
LNZ308
LNZ428
U373
0
0.7
1.5
3
6
12
25
50
100
200
400
Trichostatin A (nM)

Fig.4

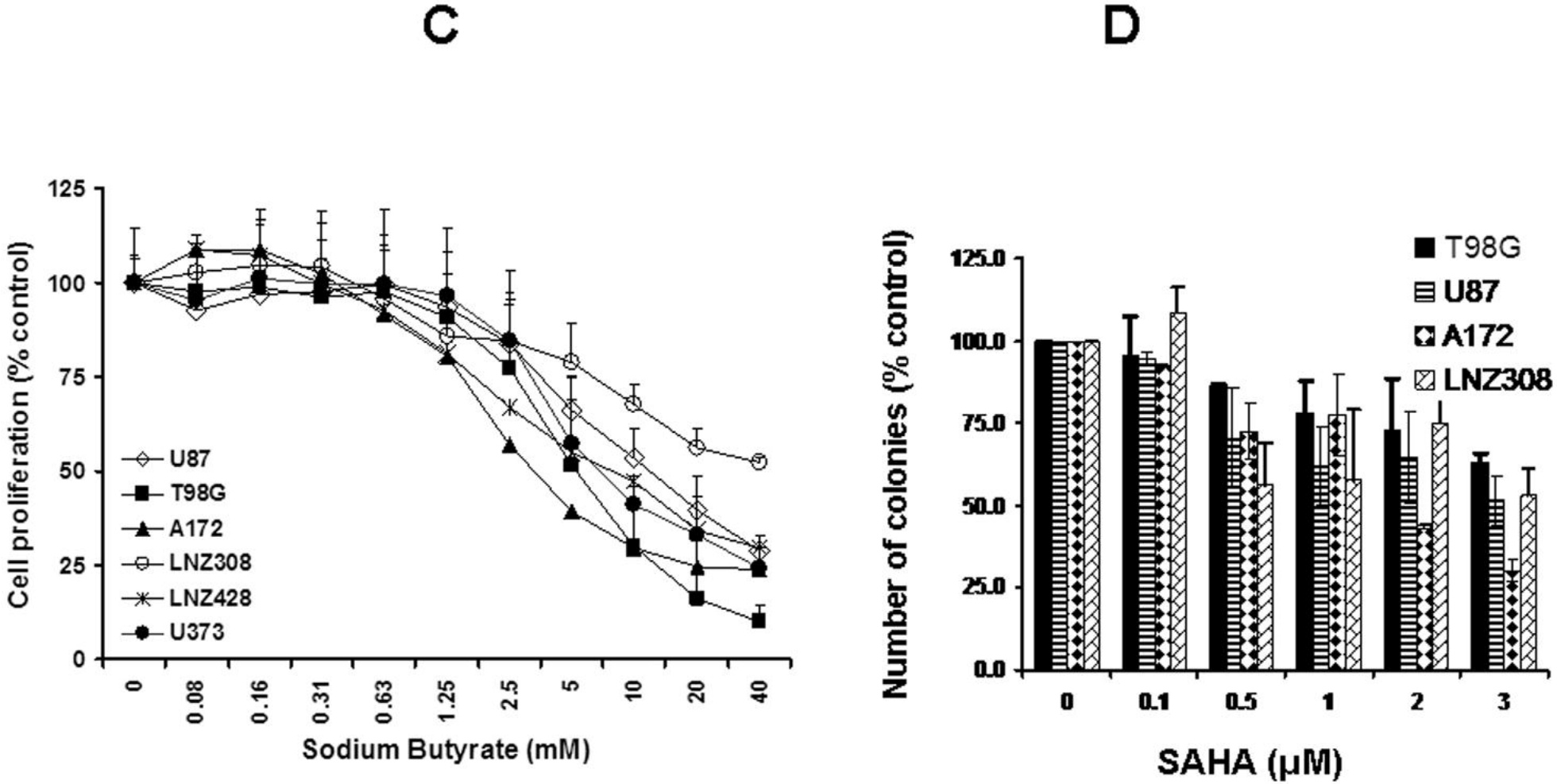
C
D
125
100
75
50
25
0
Cell proliferation (% control)
U87
T98G
A172
LNZ308
LNZ428
U373
0
0.08
0.16
0.31
0.63
1.25
2.5
5
10
20
40
Sodium Butyrate (mM)
Number of colonies (% control)
125.0
100.0
75.0
50.0
25.0
0.0
T98G
U87
A172
LNZ308
0
0.1
0.5
1
2
3
SAHA (μM)

Fig.5

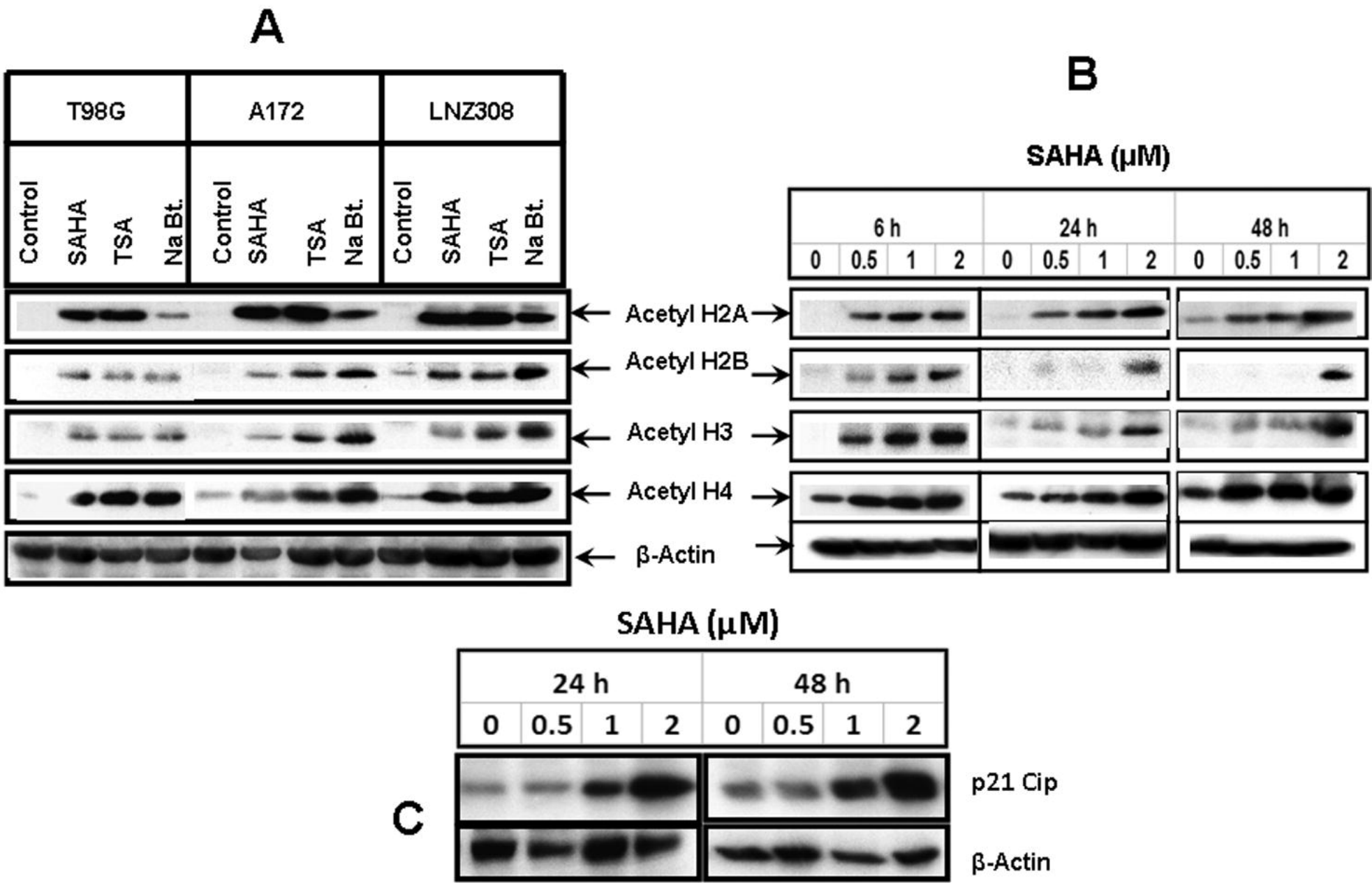
A
T98G
A172
LNZ308
Control
SAHA
TSA
Na Bt.
Acetyl H2A
Acetyl H2B
Acetyl H3
Acetyl H4
β-Actin
B
SAHA (μM)
6 h
24 h
48 h
0
0.5
1
2
C
SAHA (μM)
24 h
48 h
p21 Cip
β-Actin

Fig.6

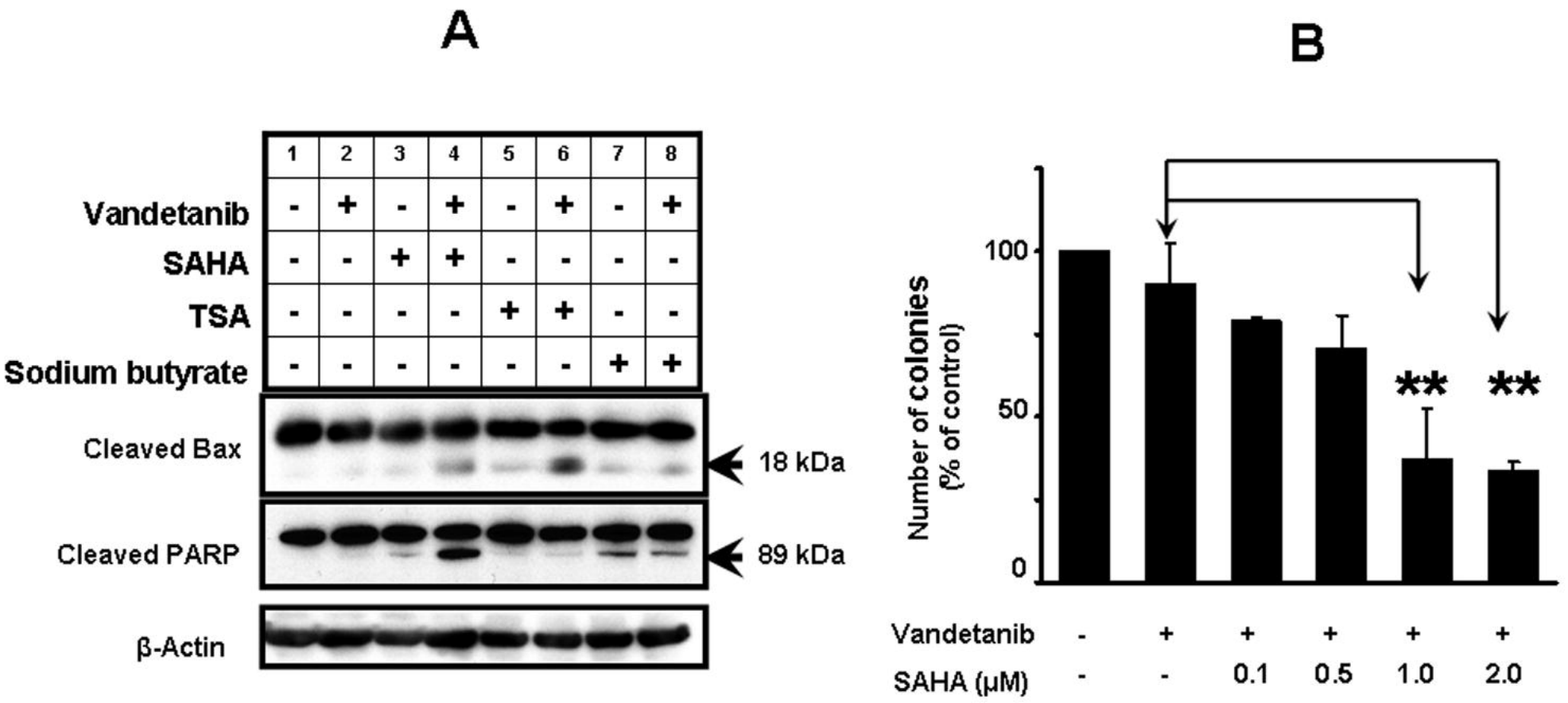
A
1 2 3 4 5 6 7 8
Vandetanib - + - + - + - +
SAHA - - + + - - - -
TSA - - - - + + - -
Sodium butyrate - - - - - - + +
Cleaved Bax
18 kDa
Cleaved PARP
89 kDa
β-Actin
B
Number of colonies (% of control)
100
50
0
**
**
Vandetanib - + + + + +
SAHA (μM) - - 0.1 0.5 1.0 2.0

Fig.7

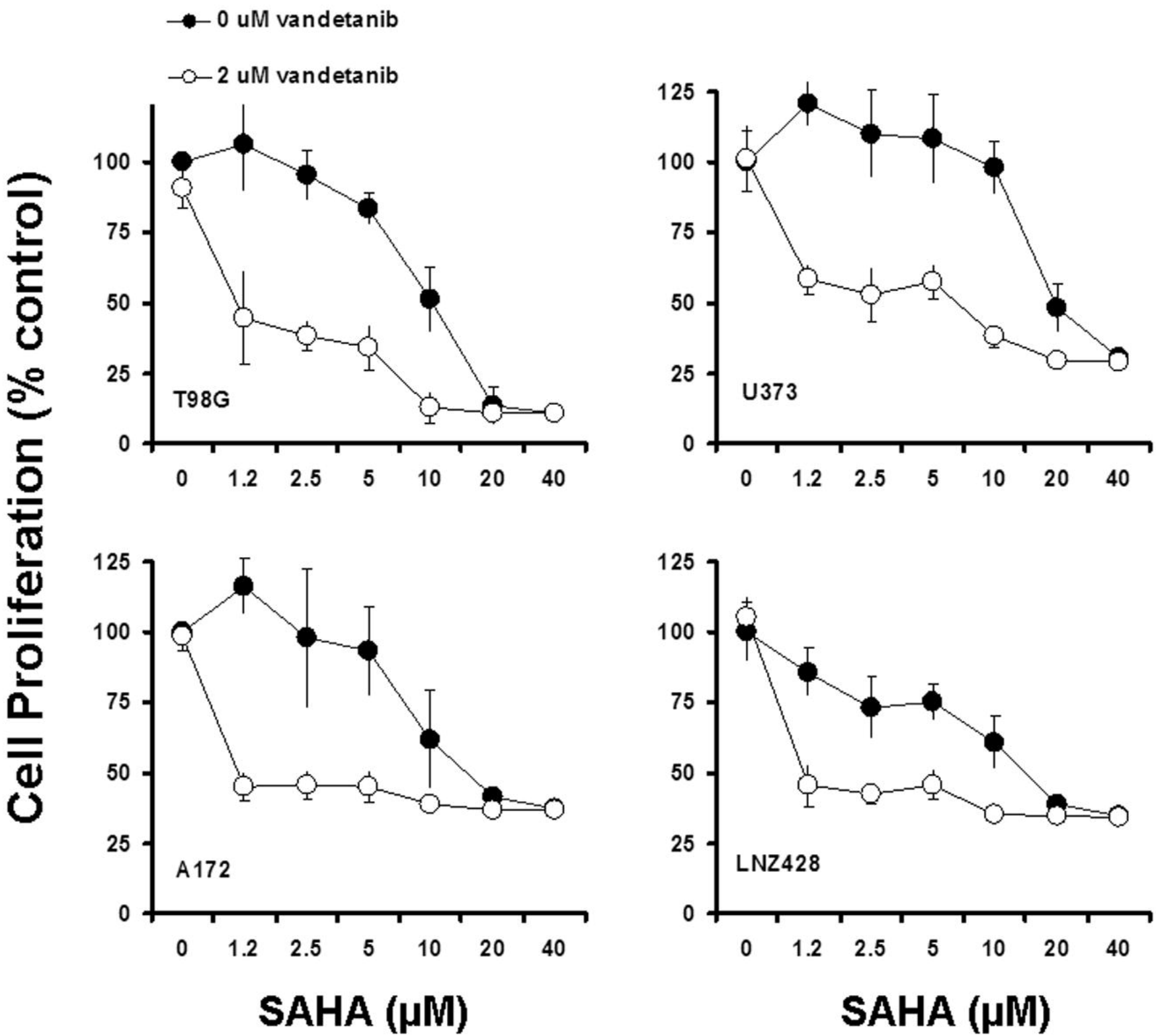
0 uM vandetanib
2 uM vandetanib
Cell Proliferation (% control)
T98G
U373
A172
LNZ428
0
25
50
75
100
125
0
1.2
2.5
5
10
20
40
SAHA (μM)
SAHA (μM)

Fig.8

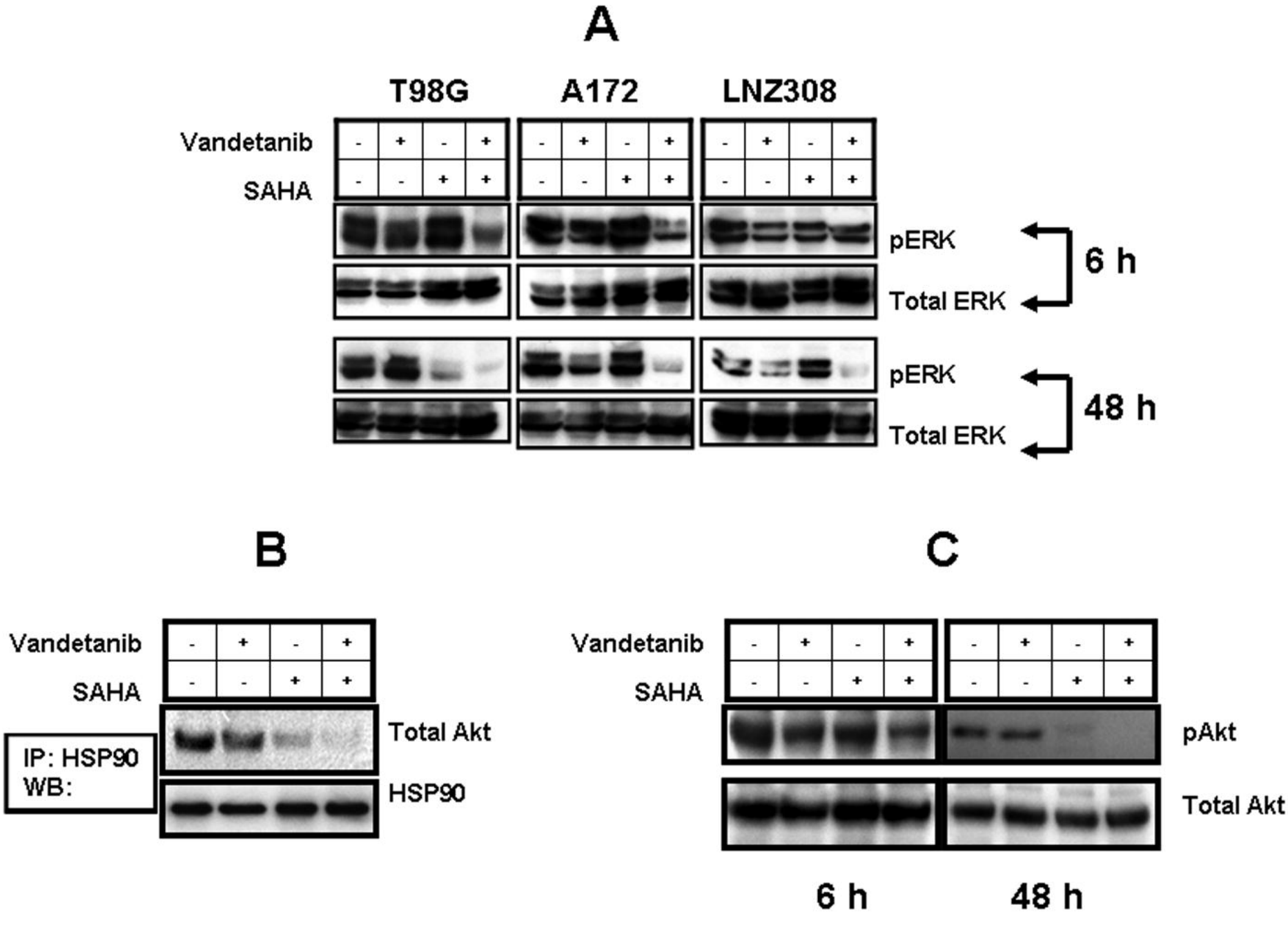
A
T98G
A172
LNZ308
Vandetanib
SAHA
pERK
Total ERK
6 h
48 h
B
IP: HSP90
WB:
Total Akt
HSP90
C
pAkt
Total Akt
6 h
48 h

Fig.8

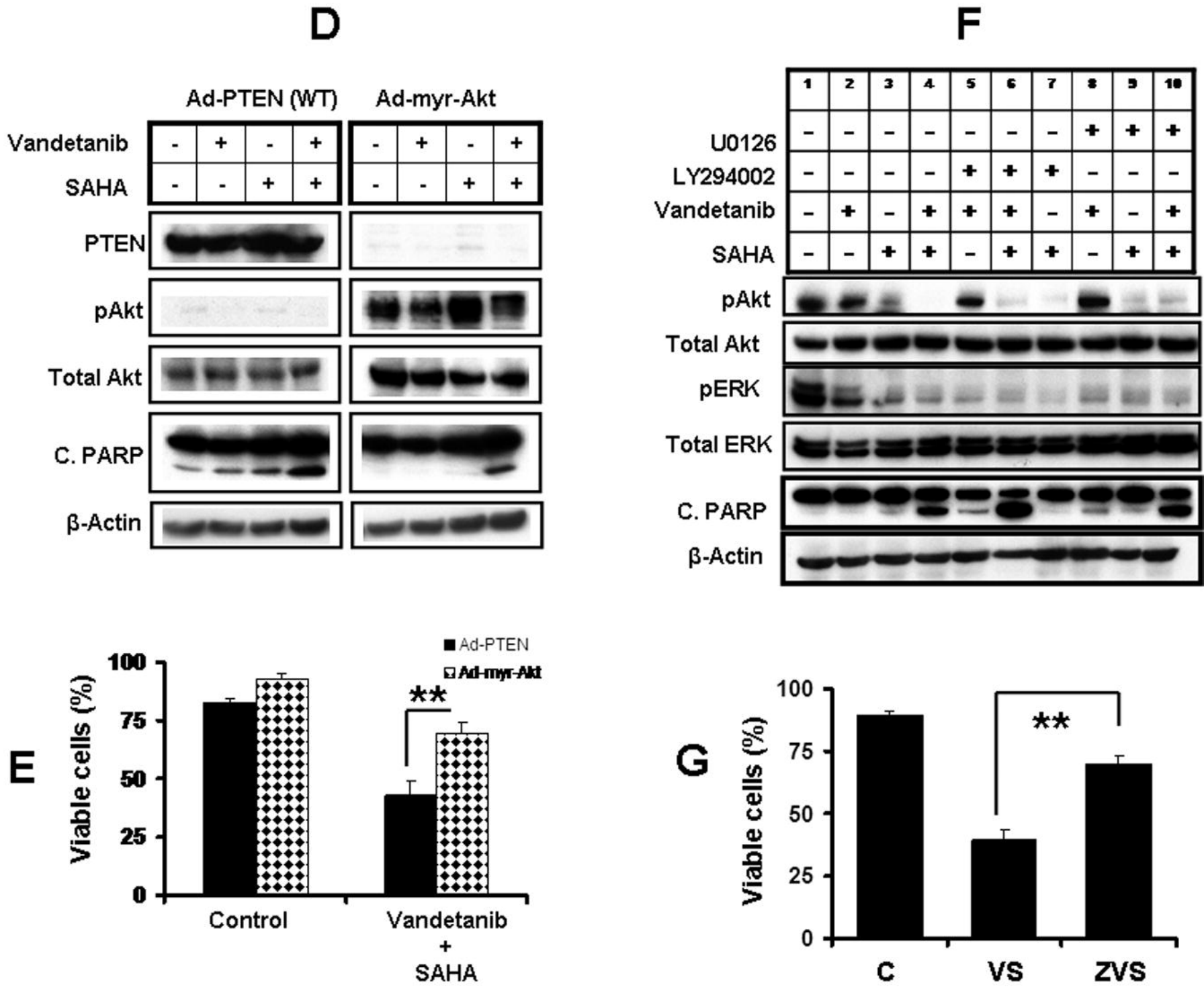
D
Ad-PTEN (WT)
Ad-myr-Akt
Vandetanib
SAHA
PTEN
pAkt
Total Akt
C. PARP
β-Actin
F
1 2 3 4 5 6 7 8 9 10
U0126
LY294002
Vandetanib
SAHA
pAkt
Total Akt
pERK
Total ERK
C. PARP
β-Actin
E
Ad-PTEN
Ad-myr-Akt
Viable cells (%)
100
75
50
25
0
**
Control
Vandetanib + SAHA
G
Viable cells (%)
100
75
50
25
0
**
C
VS
ZVS